High Coupling Efficiency Etched Facet Tapers in Silicon Waveguides

Jaime Cardenas, Carl B. Poitras, Kevin Luke, Lian-Wee Luo, Paul Adrian Morton, and Michal Lipson

***Abstract*— We demonstrate a platform based on etched facet silicon inverse tapers for waveguide-lensed fiber coupling with a loss as low as 0.7 dB/facet. This platform can be fabricated on a wafer scale enabling mass-production of silicon photonic devices with broadband, high-efficiency couplers.**

***Index Terms*— Waveguides, coupler, inverse tapers, photonics.**

THE TWO main approaches for coupling light on a high-confinement chip with submicron waveguides are gratings, which suffer from inherently low bandwidth, or taper couplers, which require one-die-at-a-time processing to achieve high coupling efficiency for end-fire coupling [1]–[28]. Grating couplers are inherently bandwidth-limited and require complex fabrication for high efficiency coupling. Most gratings show coupling loss (to/from a cleaved single mode fiber) of a few dB (∼2–6 dB) with a 3 dB bandwidth of tens of nanometers [5], [9], [11], [13], [17], [21] while complex, multi-etch gratings with bottom reflectors have reached sub-dB loss with broader bandwidth [24], [25], [27], [28]. A few other proposed approaches for grating geometries are based on transformation optics [29], [30], parabolic reflectors [31], and subwavelength grating tapers [32], [33], however they also suffer from the bandwidth-efficiency tradeoff. Most inverted couplers show lower coupling loss than gratings, typically less than 1 dB, with 3 dB bandwidth of hundreds of nanometers [1], [4], [14], [20], [24]. More complex inverse tapers using multiple coupling stages and suspended structures can reach sub-dB coupling loss for lensed fiber input and 1–2 dB for standard cleaved fibers [19], [22], [23], [26]. However, to date, taper coupler structures require one-die-at-a-time mechanical polishing to achieve smooth surfaces for high coupling efficiency. Some works have reported coupling using facet etching [7], [20], [23], [34]; but they consist of (a) multi-stage or suspended taper structures that require more complex fabrication and might be susceptible to vibrations or (b) tapers terminated directly at the etched facet [7], [34], which require a challenging etch process to avoid distortion of the taper tip and other finer features on a chip and therefore might limit its implementation in wafer scale production.

Here we show a platform for tapered waveguide coupling structures based on etched facet using a single simple etching process with high efficiency fiber-waveguide coupling suitable for fabrication on a wafer scale. The challenge in traditional etching of the waveguide facets is that the reactive ion etching process must etch through multiple materials at the same time, e.g., oxide from the cladding and silicon from the nanotaper. The different etch rate for the oxide and silicon creates artifacts that distort the silicon taper facet and lead to coupling loss. Here we overcome this challenge by terminating the silicon nanotaper with an oxide gap and etching the facet at the wafer-level to obtain a high-quality coupling interface. Instead of defining the facets of the waveguide at the end point of the taper, we leave a gap between the end of the taper and the coupling facet (Fig. 1). The gap is composed of the overcladding material, which in this case is silicon dioxide. Leaving the oxide gap ensures etching of only one material throughout the cross-section of the facet, which enables fabrication of a smooth and vertical surface for high efficiency coupling.

We show that since the optical mode is focused at the tip of the nanotaper, the effect of the oxide gap on the coupling efficiency is small. We simulate the tapered waveguides with the oxide gap etched facet using a 3D Finite Difference Time Domain (FDTD) approach and show that the oxide gap has a weak effect on the mode matching between the lensed fiber and the nanotaper. The Si waveguide is linearly tapered down from its 500 nm width to a 160 nm tip over a length of 100 μm. First we determine the launch position of the lensed optical fiber mode (working distance of 14 μm, spot size of $2.5+/-0.5$ μm) using Gaussian optics to account for the presence of the oxide gap. Then we launch the lensed optical fiber mode at the oxide-air interface such that it focuses at the correct spot size at the silicon taper tip. Propagation in the oxide gap and silicon taper is simulated with 3D FDTD. The launched fiber mode has a spherical wavefront. To calculate the coupling efficiency, we simulate the mode propagation through the taper and monitor the total

Manuscript received April 29, 2014; accepted September 3, 2014. Date of publication September 11, 2014; date of current version November 4, 2014. This work was supported in part by the Defense Sciences Office, Defense Advanced Research Projects Agency, Small Business Technology Transfer, under Contract W91CRB-10-C-0099, in part by the Cornell NanoScale Facility, a Member of the National Nanotechnology Infrastructure Network, and in part by the National Science Foundation under Grant ECCS-0335765.

J. Cardenas, C. B. Poitras, and K. Luke are with the School of Electrical and Computer Engineering, Cornell University, Ithaca, NY 14850 USA (e-mail: jc922@cornell.edu; cbp8@cornell.edu; kjl88@cornell.edu).

L.-W. Luo was with the School of Electrical and Computer Engineering, Cornell University, Ithaca, NY 14850 USA. He is now with the Institute of Microelectronics, Singapore 117685 (e-mail: ll399@cornell.edu).

P. A. Morton is with Morton Photonics Inc., West Friendship, MD 21794 USA (e-mail: pmorton@mortonphotonics.com).

M. Lipson is with the School of Electrical and Computer Engineering, Kavli Institute, Cornell University, Ithaca, NY 14850 USA (e-mail: ml292@cornell.edu).

Color versions of one or more of the figures in this letter are available online at http://ieeexplore.ieee.org.

Digital Object Identifier 10.1109/LPT.2014.2357177

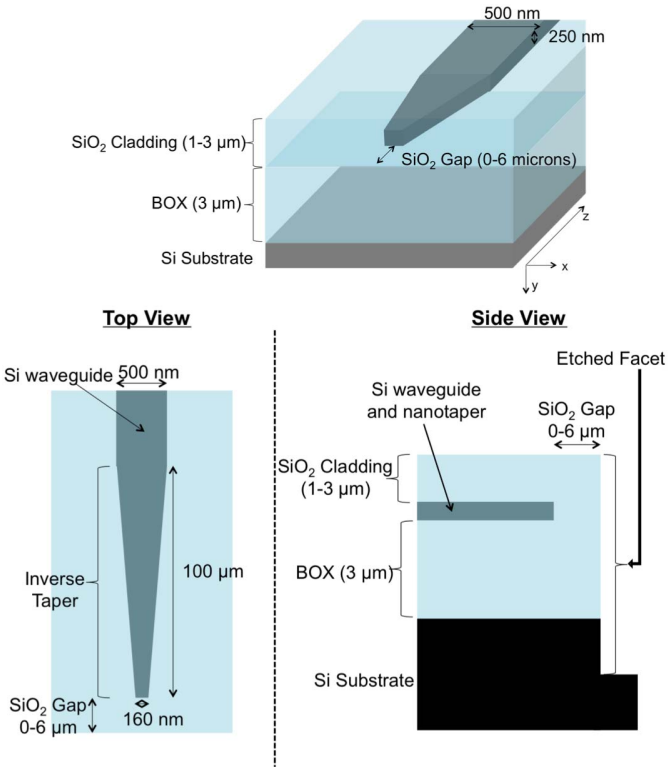

Fig. 1. Schematic of etched taper facet with oxide gap.

TABLE I
SIMULATED COUPLING LOSS FOR DIFFERENT OXIDE GAPS AND TOP OXIDE THICKNESSES

Top SiO_2	SiO_2 Gap			
	0 μm	2 μm	4 μm	6 μm
1 μm	**0.27**	**0.40**	**0.71**	**0.92**
2 μm	**0.22**	**0.40**	**0.46**	**0.51**
3 μm	**0.22**	**0.40**	**0.46**	**0.46**

power in the waveguide. As shown in Table I, the results of our simulations reveal that, for a top SiO_2 cladding that is 2 μm or greater, and an oxide gap that is 2 μm or larger, the additional coupling losses due to the presence of the oxide gap are less than 0.3 dB, indicating that the oxide gap has a weak effect on the mode matching between the lensed fiber and the nanotaper. We attribute losses in our simulations to two factors: the discretization of the 3D simulation domain (computer memory versus simulation accuracy trade-off, these losses should be constant for all simulations as the discretization does not change), and the fact that for longer oxide gaps, the optical field coming from air and hitting the air-oxide interface has a larger diameter (to ensure that the 2.5 micron spot size is at the Si taper tip), and this results in more optical field interacting with the Si substrate leading to loss. This last source of loss is especially more important when the top oxide cladding is thin ($\sim$1 micron).

To characterize the coupling loss of the etched facet nanotapers with oxide gap, we fabricate 250 nm by 500 nm

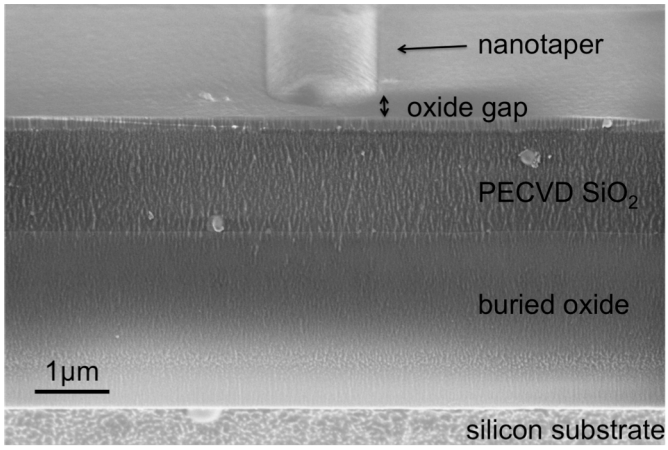

Fig. 2. SEM of etched facet inverse taper waveguide with a 2 μm oxide gap. The image was taken with a 70° tilt.

waveguides of 0.69 mm, 2.78 mm, and 4.37 mm in length, with oxide gaps ranging from 2 to 6 μm. The waveguides are patterned with e–beam lithography, etched in a chlorine chemistry and clad with 2.4 μm of PECVD silicon oxide. Then, openings are patterned using contact photolithography to define the inverse taper waveguide facets and the silicon dioxide (both the PECVD overcladding and the buried oxide) is etched in an ICP RIE using a CHF_3/O_2 chemistry. Finally the silicon substrate is deep etched using the Bosch process so that the chip facet can be accessed with a lensed fiber (see SEM of taper on Fig. 2).

We measure a coupling loss as low as 0.7 dB per facet for a nanotaper tip width of 160 nm and oxide gap of 2 μm at a wavelength of 1550 nm. Note that the inverse taper insures that only the fundamental mode is coupled into the waveguide. The coupling loss is measured using the "cut-back" method. We measure the throughput of the waveguides of different lengths and fit the results to a straight line (Fig. 3a). The point where the fitted line crosses the y-axis indicates the insertion loss of the two nanotapers. We then measure the throughput of the lensed fibers (working distance of 14 μm, spot size of $2.5+/-0.5$ μm) back-to-back (with no silicon die present) and determine that their loss is 1.6 dB. To calculate the coupling loss, we subtract the lensed fiber losses from the insertion loss measured via the "cut-back" method. This method to measure coupling losses accounts for the propagation loss in the taper itself as well as the mode matching loss to the input fiber and excludes the losses due to the fiber/lensed-fiber transition. For a 2-μm oxide gap we measured an insertion loss of 3.1 dB with a low coupling loss of 0.7 dB per facet. All devices with oxide gaps between 2 and 6 μm had a coupling efficiency within a range of 0.5 dB (Fig. 3b).

The measured low coupling loss per facet of 0.7 dB can in principle be lowered down to the theoretical value of 0.2 dB by improving the quality of the photolithography and the PECVD oxide. We show the expected coupling loss per facet in Fig. 3b (dashed line). One can see that the simulations predict even lower coupling losses. The discrepancy between the simulated values and the measured ones is mostly due to fabrication imperfections. These imperfections can be seen in Fig. 2 where the roughness is clearly visible.

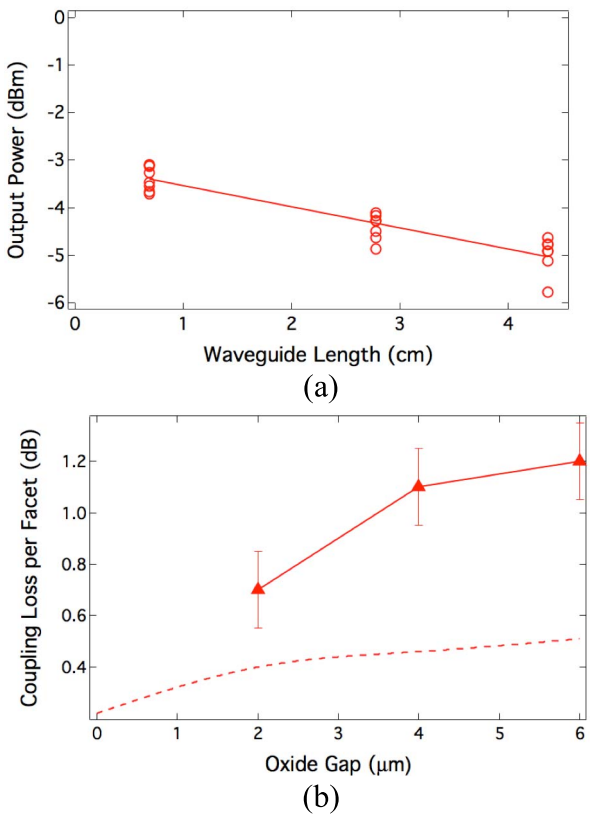

Fig. 3. (a) Output power vs. different waveguide lengths for an oxide gap of 2 μm. The insertion loss of the waveguide corresponds to the zero crossing of the straight line (solid line in graph) fitted to the data. (b) Coupling loss per facet vs. oxide gap. Solid symbols show measured data. The line is a guide to the eye. Dashed line shows simulated coupling loss versus oxide gap. The coupling loss per facet is calculated by subtracting.

REFERENCES

[1] T. Shoji, T. Tsuchizawa, T. Watanabe, K. Yamada, and H. Morita, "Low loss mode size converter from 0.3μm square Si wire waveguides to singlemode fibres," *Electron. Lett.*, vol. 38, no. 25, pp. 1669–1670, 2002.

[2] A. Sure, T. Dillon, J. Murakowski, C. Lin, D. Pustai, and D. Prather, "Fabrication and characterization of three-dimensional silicon tapers," *Opt. Exp.*, vol. 11, no. 26, pp. 3555–3561, 2003.

[3] V. R. Almeida, R. R. Panepucci, and M. Lipson, "Nanotaper for compact mode conversion," *Opt. Lett.*, vol. 28, no. 15, pp. 1302–1304, 2003.

[4] G. Roelkens, P. Dumon, W. Bogaerts, D. Van Thourhout, and R. Baets, "Efficient silicon-on-insulator fiber coupler fabricated using 248-nm-deep UV lithography," *IEEE Photon. Technol. Lett.*, vol. 17, no. 12, pp. 2613–2615, Dec. 2005.

[5] G. Z. Masanovic *et al.*, "A high efficiency input/output coupler for small silicon photonic devices," *Opt. Exp.*, vol. 13, no. 19, pp. 7374–7379, Sep. 2005.

[6] A. Delage *et al.*, "Monolithically integrated asymmetric graded and step-index couplers for microphotonic waveguides," *Opt. Exp.*, vol. 14, no. 1, pp. 148–161, Jan. 2006.

[7] K. P. Yap *et al.*, "Fabrication of lithographically defined optical coupling facets for silicon-on-insulator waveguides by inductively coupled plasma etching," *J. Vac. Sci. Technol. A*, vol. 24, no. 3, pp. 812–816, May 2006.

[8] V. Nguyen *et al.*, "Silicon-based highly-efficient fiber-to-waveguide coupler for high index contrast systems," *Appl. Phys. Lett.*, vol. 88, no. 8, pp. 081112-1–081112-3, 2006.

[9] L. Vivien *et al.*, "Light injection in SOI microwaveguides using high-efficiency grating couplers," *J. Lightw. Technol.*, vol. 24, no. 10, pp. 3810–3815, Oct. 2006.

[10] L. Vivien, X. L. Roux, S. Laval, E. Cassan, and D. Marris-Morini, "Design, realization, and characterization of 3-D taper for fiber/micro-waveguide coupling," *IEEE J. Sel. Topics Quantum Electron.*, vol. 12, no. 6, pp. 1354–1358, Nov./Dec. 2006.

[11] F. Van Laere *et al.*, "Compact focusing grating couplers for silicon-on-insulator integrated circuits," *IEEE Photon. Technol. Lett.*, vol. 19, no. 23, pp. 1919–1921, Dec. 1, 2007.

[12] A. Harke, T. Lipka, J. Amthor, O. Horn, M. Krause, and J. Muller, "Amorphous silicon 3-D tapers for Si photonic wires fabricated with shadow masks," *IEEE Photon. Technol. Lett.*, vol. 20, no. 17, pp. 1452–1454, Sep. 1, 2008.

[13] X. Chen, C. Li, and H. K. Tsang, "Fabrication-tolerant waveguide chirped grating coupler for coupling to a perfectly vertical optical fiber," *IEEE Photon. Technol. Lett.*, vol. 20, no. 23, pp. 1914–1916, Dec. 1, 2008.

[14] A. Barkai *et al.*, "Double-stage taper for coupling between SOI waveguides and single-mode fiber," *J. Lightw. Technol.*, vol. 26, no. 24, pp. 3860–3865, Dec. 15, 2008.

[15] H. Yoda *et al.*, "A two-port single-mode fiber–silicon wire waveguide coupler module using spot-size converters," *J. Lightw. Technol.*, vol. 27, no. 10, pp. 1315–1319, May 15, 2009.

[16] J. Bolten *et al.*, "CMOS compatible cost-efficient fabrication of SOI grating couplers," *Microelectron. Eng.*, vol. 86, nos. 4–6, pp. 1114–1116, 2009.

[17] T. Wahlbrink *et al.*, "Fabrication of high efficiency SOI taper structures," *Microelectron. Eng.*, vol. 86, nos. 4–6, pp. 1117–1119, 2009.

[18] Y. Liu, X. Xu, B. Xing, Y. Yu, and J. Yu, "Fabrication of a low-loss SSC using high-dose electron beam lithography exposure with negative PMMA resist," *IEEE Photon. Technol. Lett.*, vol. 22, no. 7, pp. 501–503, Apr. 1, 2010.

[19] Q. Fang *et al.*, "Suspended optical fiber-to-waveguide mode size converter for silicon photonics," *Opt. Exp.*, vol. 18, no. 8, pp. 7763–7769, Apr. 2010.

[20] M. Pu, L. Liu, H. Ou, K. Yvind, and J. M. Hvam, "Ultra-low-loss inverted taper coupler for silicon-on-insulator ridge waveguide," *Opt. Commun.*, vol. 283, no. 19, pp. 3678–3682, 2010.

[21] X. Xiao *et al.*, "Wafer-level testable high-speed silicon microring modulator integrated with grating couplers," *Chin. Phys. Lett.*, vol. 27, no. 9, p. 094207, 2010.

[22] L. Chen, C. R. Doerr, Y.-K. Chen, and T.-Y. Liow, "Low-loss and broadband cantilever couplers between standard cleaved fibers and high-index-contrast Si_3 N_4 or Si waveguides," *IEEE Photon. Technol. Lett.*, vol. 22, no. 23, pp. 1744–1746, Dec. 1, 2010.

[23] C. Liao, Y. Yang, S. Huang, and M. M. Lee, "Fiber-core-matched three-dimensional adiabatic tapered couplers for integrated photonic devices," *J. Lightw. Technol.*, vol. 29, no. 5, pp. 770–774, Mar. 1, 2011.

[24] C. Kopp *et al.*, "Silicon photonic circuits: On-CMOS integration, fiber optical coupling, and packaging," *IEEE J. Sel. Topics Quantum Electron.*, vol. 17, no. 3, pp. 498–509, May 2011.

[25] A. Mekis *et al.*, "A grating-coupler-enabled CMOS photonics platform," *IEEE J. Sel. Topics Quantum Electron.*, vol. 17, no. 3, pp. 597–608, May 2011.

[26] M. Wood, P. Sun, and R. M. Reano, "Compact cantilever couplers for low-loss fiber coupling to silicon photonic integrated circuits," *Opt. Exp.*, vol. 20, no. 1, pp. 164–172, Jan. 2012.

[27] X. Xu, H. Subbaraman, J. Covey, D. Kwong, A. Hosseini, and R. T. Chen, "Complementary metal–oxide–semiconductor compatible high efficiency subwavelength grating couplers for silicon integrated photonics," *Appl. Phys. Lett.*, vol. 101, no. 3, p. 031109, 2012.

[28] W. S. Zaoui *et al.*, "Bridging the gap between optical fibers and silicon photonic integrated circuits," *Opt. Exp.*, vol. 22, no. 2, pp. 1277–1286, Jan. 2014.

[29] L. H. Gabrielli and M. Lipson, "Integrated Luneburg lens via ultra-strong index gradient on silicon," *Opt. Exp.*, vol. 19, no. 21, pp. 20122–20127, Oct. 2011.

[30] P. Markov, J. G. Valentine, and S. M. Weiss, "Fiber-to-chip coupler designed using an optical transformation," *Opt. Exp.*, vol. 20, no. 13, pp. 14705–14713, Jun. 2012.

[31] T. Dillon, J. Murakowski, S. Shi, and D. Prather, "Fiber-to-waveguide coupler based on the parabolic reflector," *Opt. Lett.*, vol. 33, no. 9, pp. 896–898, May 2008.

[32] J. H. Schmid *et al.*, "Subwavelength grating structures in silicon-on-insulator waveguides," *Adv. Opt. Technol.*, vol. 2008, p. 685489, May 2008.

[33] P. Cheben *et al.*, "Refractive index engineering with subwavelength gratings for efficient microphotonic couplers and planar waveguide multiplexers," *Opt. Lett.*, vol. 35, no. 15, pp. 2526–2528, Aug. 2010.

[34] A. E.-J. Lim *et al.*, "Review of silicon photonics foundry efforts," *IEEE J. Sel. Topics Quantum Electron.*, vol. 20, no. 4, Jul. 2014, Art. ID 8300112.